STEPPED-FMCW WAVEFORM APPLIED FOR MM-WAVE AUTOMOTIVE COLLISION WARNING RADAR

ZHANG Jian-Hui LIU Guo-Sui GU Hong SU Wei-Min
(RCEET of Nanjing University of Science and Technology, Nanjing, Jiangsu 210094, China)

Abstract A stepped-FMCW radar waveform applied for mm-wave automotive collision warning radar systems was proposed, which is easy to be generated digitally and its signal processing reduced the requirement of computational speed compared to conventional hgih-resolution radars. An error approach algorithm was suggested for multiple vehicle target detection and its usefulness in eliminating the false target by computer simulation was confirmed.
Key words stepped-FMCW, automotive radar, false alarm rate, target detection.

步进调频连续波信号应用于毫米波汽车防撞雷达

张建辉 刘国岁 顾 红 苏卫民
(南京理工大学电子工程技术研究中心, 江苏, 南京, 210094)

摘要 概述了工作在毫米波段的汽车防撞雷达的有关情况, 针对虚警问题, 提出了一种新的雷达发射信号体制, 即变斜率步进调频三角形连续波信号, 分析了该波形的特性, 给出了其相应的信号处理, 并提出了一种用于多目标环境中的目标检测算法. 分析和仿真结果表明, 新的信号体制具有良好的距离和相对速度分辨率, 且易于产生和处理, 同时其相应的多目标检测算法能够有效地去除虚警.
关键词 步进调频连续波, 汽车雷达, 虚警率, 目标检测

Introduction

From a relative view point, road traffic is one of the dangerous means of transportation. Statistic of accidents shows that more than half of all collisions are rear-end collisions[1]. So it is believed by people that a system capable of alerting a driver in a timely fashion to the existing of an impending collision would have the potentiality of drastically reducing accident seriousness as well as frequency. With those systems the car driver's stress will be reduced and car driving will be more relaxing and comfortable. High resolution radars operating on millimeter-wave band are the ideal sensors for these systems[2,3].

In history radar systems in car applications were developed, which were named "Forward Looking Automotive Collision Warning Radar (FLAR)". Modern developments are focused on the so-called "Autonomous Intelligent Cruise Control Systems (AICC)"[4,5], which means in addition to the collision warning systems the car's brake and accelerations are controlled automatically by the radar system including a traffic analyzing computer. The collisions will be avoided totally by the AICC-computer.

Although many radar prototypes have been produced[1,4~7], and relative results or papers have been published, to date, however, no truly effective system has been developed and marketed. Except the consideration of the cost, the principal reason is the unacceptably high false alarm rates.

Received 2000-01-24, revised 2000-03-27
稿件收到日期 2000-01-24, 修改稿收到日期 2000-03-27

The low false alarm rate puts tough demands on radar sensor, so for whether FLAR or AICC systems, the predominant task is to design a radar system with small false-to-real hazard detection ratio. People have realized, to get low false alarm rates, radar system must be able to measure the three parameters of the target simultaneously, they are range, velocity and azimuth angle. Each of these parameters can be obtained by many different means based upon the transmit waveform and antenna selected.

In this paper, a complex waveform applied for FLAR or AICC, with its signal processing algorithm for target detection is proposed. The waveform can offer high resolution and the target detection algorithm provides good capability in eliminating the false target.

1 Waveform and Signal Processing

1.1 Waveform definition

Radar detection basically depends on the transmission signal waveform. In Fig. 1 a new waveform (stepped-FMCW) applied for FLAR or AICC is shown. It includes three slope pairs and can be divided into six segments, A - F, in one cycle. Segments A, C and E correspond to the classic upchirp, and B, D, F, downchirp, where f_c is the carrier frequency. However, the frequency is not tuned continuously. Every segment comprises N steps of short bursts and the duration of each burst is T_p, each of them having a constant frequency. In addition, the frequency spacing ΔF for each slope pair (A,B), (C,D), and (E,F) is different.

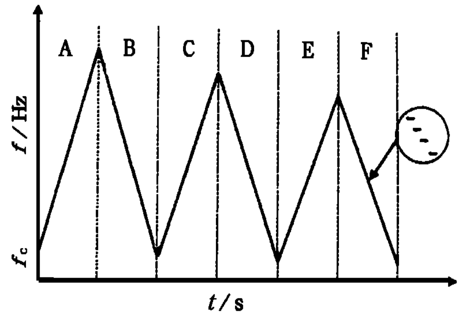

Fig. 1 Waveform design of the transmission signal in one cycle
图1 发射波形一个周期的示意图

Figure 2 shows the waveform of the bursts that comprised segment A and segment B, where A_p represents the amplitude of bursts. The advantages of this stepwise coded frequencies strategy are firstly, the simple digital generation of the modulation signal and secondly the reflected signals coming in are mixed with the constant frequency of the actually transmitted burst. At the end of each burst, when possible VCO or mixer transients are settled, the mixer output signals are sampled (Fig. 3). Thirdly, using this waveform, we can easily calculate the range and velocity of every vehicle target in the front of the radar sensor. Furthermore, the step-by-step operation makes it easier to digitally calibrate the system.

1.2 Signal processing

When the signal of segment A is transmitted, the received signal from a target is homodynely detected into a train of base-band pulses and then I-Q sampled at a rate of Pulse-Repetition Interval (PRI) T_p. Then the sample at the i-th (i= 0, 1, 2,... ,N - 1) frequency step is given by

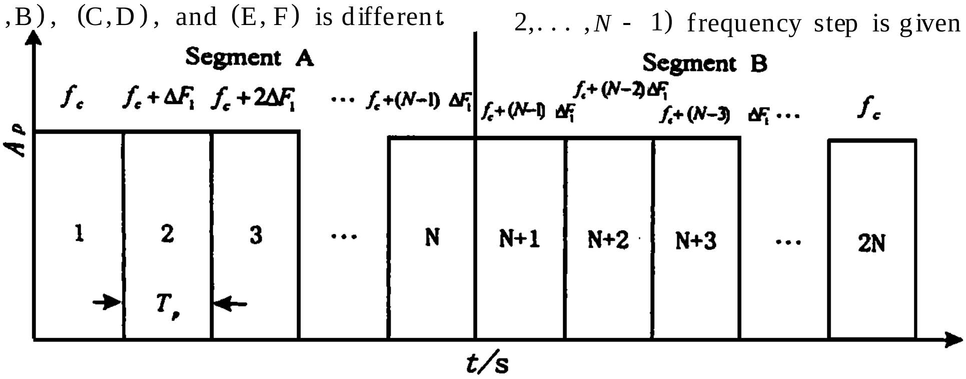

Fig. 2 The waveform of bursts comprising segment A and segment B
图2 A段和B段脉冲串示意图

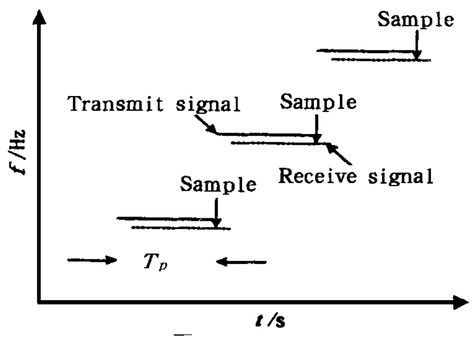

Fig. 3 Definition of the sample point of the received signal

图 3　回波信号采样时刻示意图

$$R(i) = A_i \exp[-j2\pi(f_c + i\Delta F_1)\tau(i)], \quad (1)$$

$$\tau(i) = \frac{2(d + ivT_p)}{c}, \quad (2)$$

where A_i is the amplitude of the i-th pulse, $f_c + i\Delta F_1$ is the transmitted RF frequency, $\tau(i)$, the range delay for the target, v, the relative velocity of the target, and d, an initial range at $i = 0$.

According to Refs [8, 9], for all samples, $R(i)$ is then applied to the IDFT in order to obtain an N-element synthetic radar profile as follows:

$$S(\phi) = \left|\sum_{i=0}^{N-1} R(i)\exp\left(\frac{j2\pi i\phi}{N}\right)\right| = \left|\sum_{i=0}^{N-1}\exp\left(-\frac{j4\pi i\phi}{c}\right)\right| \quad (3)$$

where

$$\phi = df_c + i\left(\Delta F_1 d + f_c T_p v - \frac{c\phi}{2N}\right) + i^2 v T_p \Delta F_1. \quad (4)$$

In fact, the third term of Eq. (4), which is called the Doppler and step frequency coupling, can be designed to be small as compared to other terms. For example, for a transmitted radar waveform of $f_c = 77$GHz, $\Delta F = 1$MHz and $T_p = 10\mu$s, the effect of the coupling is very small.

Then Eq. (4) can be approximated by:

$$\phi = df_c + i\left(\Delta F_1 d + f_c T_p v - \frac{c\phi}{2N}\right) \quad (5)$$

Suppose there is a point target at the range of d, then, a correlation peak, corresponding to the target position, appears at the following position:

$$\phi_0 = \frac{2N(\Delta F_1 d + f_c T_p v)}{c} + k_0 N \quad (6)$$

where $k_0 \in \{0, \pm 1, \pm 2, \ldots\}$, which is owing to the holding caused by the IDFT.

You can see that it is a difficult task to estimate d and v from Eq. (6). In order to determine the d and v, we need another equation.

In segment B, similar to segment A, the correlation peak appears at the following position:

$$\bar{\phi}_0 = \frac{2N(-\Delta F_1 d + f_c T_p v)}{c} + \bar{k}_0 N \quad (7)$$

where $\bar{k}_0 \in \{0, \pm 1, \pm 2, \ldots\}$.

It is clear that from Eq. (6) and Eq. (7), the d and v of a moving target can be determined easily, which is given by:

$$d = \frac{c(\phi_0 - \bar{\phi}_0)}{4N\Delta F_1} - \frac{c(k_0 - \bar{k}_0)}{4\Delta F}, \quad (8)$$

$$v = \frac{c(\phi_0 + \bar{\phi}_0)}{4N f_c T_p} - \frac{c(k_0 + \bar{k}_0)}{4 f_c T_p} \quad (9)$$

where the second term of Eq. (8) and Eq. (9) is mainly determined by the radar parameters such as ΔF and T_p. Assume a transmitted radar waveform of $N = 128$, $\Delta F = 1$MHz, $T_p = 10\mu$s and a moving vehicle target ahead of the host vehicle, for example, $k_0 - \bar{k}_0 = 0$ when $\phi_0 \geq \bar{\phi}_0$ and $k_0 - \bar{k}_0 = -1$ when $\phi_0 < \bar{\phi}_0$.

Similar to the first slope pair which comprises segments A and B, it is easy to understand that the other two slope pairs can also determine the d and v of a moving target.

Figure 4 shows the radar profile for various values of ΔF applied to segment A, where $d = 70$m, $v = 29$km/h, $N = 128$, $T_p = 10\mu$m, $f_c = 77$GHz, and 128 points are used in the IDFT calculation, and ΔF is 0.25MHz, 0.5MHz and 1MHz, respectively. In the figure, A represents the normalized amplitude. It is seen that the range resolution along the radar profile is inversely proportional to the total bandwidth ($N\Delta F$) of the transmitted RF pulses within each segment.

Please note that because in each slope pair (A, B), (C, D) and (E, F), the applied frequency spacing ΔF is different, the d and v of a target detected by each slope pair will be different correspondingly, that will have bad effect on the multi-

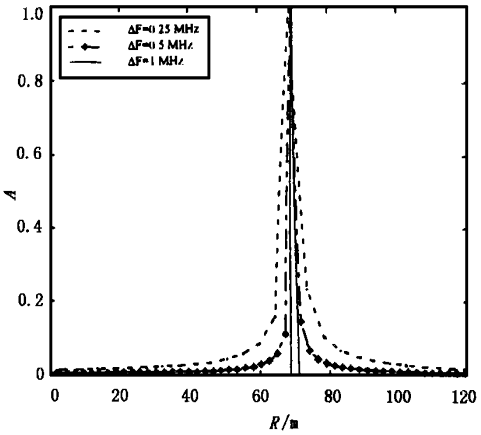

Fig. 4 The radar profile of a target
(128 points DFT)
图 4　一个目标的雷达复合距离像
(128 点 DFT)

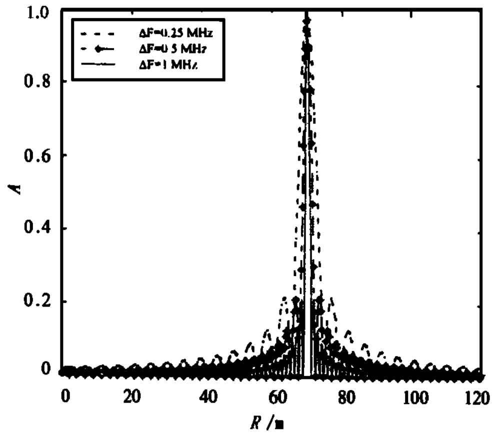

Fig. 5 The radar profile of a target
(1024 points DFT)
图 5　一个目标的雷达复合距离像
(1024 点 DFT)

ple target detection capability of the radar sensor. In fact, we can do multiple points DFT to the obtained $R(i)$ in each segment in order to make every Φ_0 or $\overline{\Phi}_0$ obtained from the DFT more approximate to the real position of the correlation peaks. In this way, the error values of the detected d and v of a target between each slope pair will be reduced to an acceptable degree. Figure 5 shows the radar profile of a moving target obtained through 1024 points DFT, the target and all other parameters are the same as in Fig. 4. Obviously, the detection precision has been improved.

2 Multiple Target Detection Algorithm

In true environment, the FLAR or AICC systems must be able to detect the d and v of every target present in the front of the host vehicle simultaneously, and then combine them with the azimuth angle information gained by antenna, to delete the false target and contain the truth. At last, by comparing every target's range d with the safety range a_s, once the interval range between the target and host vehicle advanced a_s, then there should be an alarm to the driver.

The safety range can be calculated by the following equation[9, 10]:

$$a_s = \frac{1}{2b_2}v_2^2 - \frac{1}{2b_1}v_1^2 + v_2 T_R, \tag{10}$$

where T_R is the driver's reaction time, v_1 and v_2 are the velocity of the target and the host vehicle, respectively, b_1 and b_2 are the acceleration velocity of the target and the host vehicle, respectively.

If multiple targets are present, a trial and error approach algorithm can be taken to detect the d and v of every target. According to the signal processing analyzed above, each target would contribute a Φ_0 and a $\overline{\Phi}_0$ in the result of DFT in every slope pair. For n targets, there are $2n$ variables, and n correlation peaks in each frequency modulation slope. For example, if there are three targets, then to the first slope pair, segment A and segment B are comprised, three Φ_0 and three $\overline{\Phi}_0$ will be produced in segement A and segment B, respectively, each Φ_0 is combined with each $\overline{\Phi}_0$ and nine possible targets are produced each with a d and v. So all the three slope pairs produce twenty-seven possible targets.

In fact, the three real targets will appear in each slope pair, so when all possible targets are listed, we can do comparison within them. At first, compare each possible target in the first slope pair with each possible target in the second slope pair to find data pairings that match over four slopes and have the same d, v and return power, these targets are stored as suspects and the undesirable data pairings then can be eliminated. In the next step, the remaining data pairings are compared to the possible target in the third slope pair. When all comparisons are completed, the data pairing that matches all the slopes is stored as the real target, and safety range is calculated for each one. Once the actual distance d is less than the safety range a_s, an alarm signal is produced.

The algorithm presented above can be understood in another way. In fact, the Eq. (6) can be written as:

$$v = -\frac{\Delta F_1}{P}d + Q \qquad (11)$$

where

$$P = f_c T_p, Q = \frac{(c\phi_0 - k_0 N)}{2N f_c T_p}$$

The Eq. (11) represents diagonal line LA in a diagram of relative speed versus range. Similarly, LB to LF which corresponds to segment B to segment F can be drawn, and is illustrated in Fig. 6.

Obviously, the slope of each diagonal line is determined by the frequency spacing ΔF, and Q determined by different ϕ_0 which is caused by different target. So, when all the ϕ_0's in segments A to F are calculated, the algorithm is used to test whether occurs the situation that all six lines have a common intersection, and if this is the case, the resulting target range and speed values must have the reasonable values, otherwise the intersection is rejected.

As far as the requirement of real time processing is concerned, since the DFT operation of each segment is conducted based on a rate of the PRI, the computational speed is relaxed drastically relative to conventional high-resolution radars. With the high-speed digital processor today, the time for multiple target detection can be controlled in the order of millisecond, that's sufficient for the real time processing.

Figure 6 shows a single target situation. As it can be seen, line LA and line LB would be already sufficient to calculate the range and speed of a target. However, the condition that all six lines must intersect at a reasonable position decreases the probability of false intersections (called false targets), and is particularly helpful in those multi-target situations.

Figure 7 shows the simulation result of the above algorithm, where six targets are presumed. Their ranges are 40m, 100m, 100m, 140m, 60m and 120m, respectively, and velocities are 2m/s, 2m/s, 16m/s, 20m/s, 30m/s and 10m/s, respectively. Other parameters are f_c = 77GHz, T_p = 10μs, N = 128, and 1024 points of FFT algorithm are used in the DFT calculation. When do simulations, range error is settled by 1m and velocity error, 0.2m/s, that means, when two data pairings are compared with each other, if their range error is within 1m and velocity error within 0.2m/s, then treat them as a same target. Finally, treat the average value of the three d values detected by the three slope pairs as the distance of a target, the v treated just like the d. Obviously, the six real targets were detected and no false target produced by

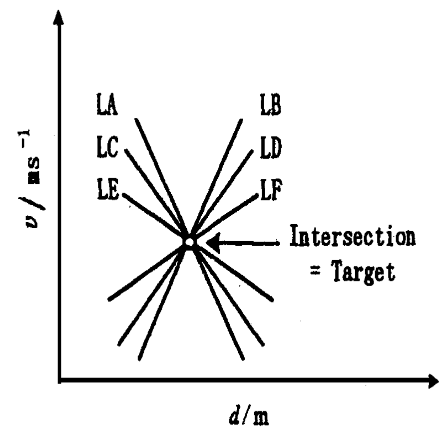

Fig. 6 Intersection finder
图 6　交叉寻找示意图

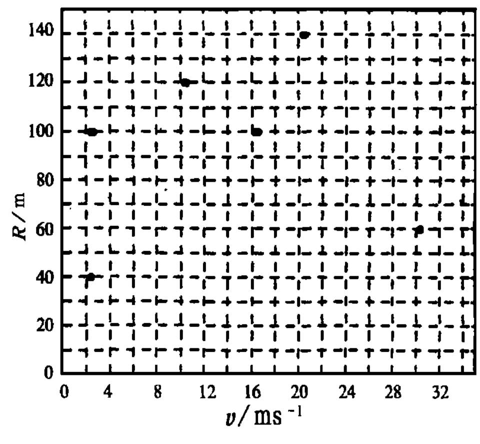

Fig. 7 Simulation result of the multi-target detection
图 7　多目标检测仿真结果示意图

the signal processing appeared.

3 Conclusion

In this paper, a stepped-FMCW radar waveform applied for mm-wave automotive collision warning radar systems is proposed. It is easy to be generated digitally and its signal processing reduced the requirement of computational speed compared to conventional high-resolution radars. We also suggested an error approach algorithm for multiple vehicle target detection and confirmed its usefulness in eliminating false targets by computer simulation.

Anyway, transmit waveform designs are critical to the viability of microwave radars, and high false alarm rate is a problem that must be overcome before the automotive collision warning radar systems can be marketed as a commercial product.

REFERENCES

[1] Rohling H, Meinecke M M, Klotz M, *et al*. Experiences with an experimental car controlled by a 77GHz radar sensor, *Proc. International Radar Symposium* 98, Munich, Germany, 1998, 345—354

[2] Grimens Dale M, Jones Trevor Owen. Automotive radar: a brief review, *Proceedings of IEEE*, 1974, **62** (6): 804—822

[3] Raffaelli Lamberto. Millimeter-wave automotive radars and related technology, *IEEE MTT-S Digest*, 1996, 35—38

[4] Winner Hermann, Witte Stefan, Uhler Werner, *et al*. Adaptive cruise control system aspects and development trends, *SAE*, *Paper* 961010, 1996

[5] Eriksson L H, *et al*. High performance automotive radar, *IEEE AES Magazine*, 1995, **10**(12): 13—18

[6] Woll Jerry D. VORAD collision warning radar, *IEEE International Radar Conference*, 1995, 369—372

[7] Detlefsen J, Schmidhammer E, Troll T. Collision warning radar using PN-code-modulation and wavefront reconstruction, *Proc. International Radar symposium* 98, Munich, Germany, 1998, 363—370

[8] Wehner Donald R. *High Resolution Radar*, Bosten: Artech House, 2nd edition, 1995

[9] Akihiro Kajiwara. Vehicular stepped-FM coded radar for collision avoidance, *Proc, IEEE* 49*th Vehicular Technology Conference*, 1998, 2085—2089

[10] Ulke Walter, Adomat Rolf, Butscher Karlheinz. Radar based automotive obstacle detection system, *SAE*, *Paper* 940904